Doc2b Protects β-Cells Against Inflammatory Damage and Enhances Function

Arianne Aslamy,[1,2] Eunjin Oh,[1] Erika M. Olson,[1] Jing Zhang,[1] Miwon Ahn,[1] Abu Saleh Md Moin,[1] Ragadeepthi Tunduguru,[1,3] Vishal A. Salunkhe,[1] Rajakrishnan Veluthakal,[1] and Debbie C. Thurmond[1,2]

Diabetes 2018;67:1332–1344 | https://doi.org/10.2337/db17-1352

Loss of functional β-cell mass is an early feature of type 1 diabetes. To release insulin, β-cells require soluble *N*-ethylmaleimide–sensitive factor attachment protein receptor (SNARE) complexes, as well as SNARE complex regulatory proteins like double C2 domain–containing protein β (Doc2b). We hypothesized that Doc2b deficiency or overabundance may confer susceptibility or protection, respectively, to the functional β-cell mass. Indeed, Doc2b$^{+/-}$ knockout mice show an unusually severe response to multiple-low-dose streptozotocin (MLD-STZ), resulting in more apoptotic β-cells and a smaller β-cell mass. In addition, inducible β-cell–specific Doc2b-overexpressing transgenic (βDoc2b-dTg) mice show improved glucose tolerance and resist MLD-STZ–induced disruption of glucose tolerance, fasting hyperglycemia, β-cell apoptosis, and loss of β-cell mass. Mechanistically, Doc2b enrichment enhances glucose-stimulated insulin secretion (GSIS) and SNARE activation and prevents the appearance of apoptotic markers in response to cytokine stress and thapsigargin. Furthermore, expression of a peptide containing the Doc2b tandem C2A and C2B domains is sufficient to confer the beneficial effects of Doc2b enrichment on GSIS, SNARE activation, and apoptosis. These studies demonstrate that Doc2b enrichment in the β-cell protects against diabetogenic and proapoptotic stress. Furthermore, they identify a Doc2b peptide that confers the beneficial effects of Doc2b and may be a therapeutic candidate for protecting functional β-cell mass.

In the U.S., type 1 diabetes currently affects an estimated 1.25 million people, and its prevalence is predicted to rise to 5 million Americans by 2050 (1–3). Type 1 diabetes is characterized by hyperglycemia caused by autoimmune destruction of islet β-cells, leading to a decline in β-cell function and mass. Increasing evidence shows that β-cell dysfunction precedes the clinical onset of type 1 diabetes (4,5). Indeed, multiple clinical trials show that patients with type 1 diabetes who display even minimal β-cell function at the onset of the study exhibit decreased microvascular complications, including retinopathy and neuropathy (6,7). Currently, the only therapy for patients with type 1 diabetes is exogenous insulin replacement. The danger in this approach, however, is that normal, glucose-dependent release of endogenous insulin is lost and that life-threatening hypoglycemic episodes and progressive destruction of β-cell mass persist. Thus, there is a high demand for alternate/adjuvant therapies that can preserve β-cell mass and function.

Normal β-cell function/insulin secretion is dependent on intact insulin secretory machinery, termed the soluble *N*-ethylmaleimide–sensitive factor attachment protein receptor (SNARE) complex. The SNARE complex consists of two target membrane (t-SNARE) proteins, syntaxin (STX) and SNAP25, and one vesicle-associated (v-SNARE) protein, VAMP (8–11). Upon glucose stimulation, one v-SNARE binds with two cognate t-SNARE proteins in a 1:1:1 heterotrimeric ratio (9). SNARE proteins facilitate biphasic insulin secretion using different requisite SNARE protein isoforms (12,13). The first phase of insulin secretion (first 5–10 min after glucose stimulation) uses STX1A, STX4, SNAP25 or SNAP23, and the v-SNARE VAMP2, whereas second-phase insulin secretion (>10 min after

[1]Department of Molecular and Cellular Endocrinology, Diabetes and Metabolic Research Institute, Beckman Research Institute of City of Hope, Duarte, CA
[2]Department of Cellular and Integrative Physiology, Indiana University School of Medicine, Indianapolis, IN
[3]Department of Diabetes Complications and Metabolism, Diabetes and Metabolic Research Institute, Beckman Research Institute of City of Hope, Duarte, CA
Corresponding author: Debbie C. Thurmond, dthurmond@coh.org.

Received 7 November 2017 and accepted 9 April 2018.

This article contains Supplementary Data online at http://diabetes.diabetesjournals.org/lookup/suppl/doi:10.2337/db17-1352/-/DC1.

J.Z. and M.A. contributed equally to this study.

glucose stimulation) uses STX4, SNAP25 or SNAP23, and VAMP2 (11,14–19). Another v-SNARE protein, VAMP8, also functions in insulin secretion and is selectively required for glucagon-like peptide 1 (GLP-1)–enhanced insulin release (20). Assembly of the β-cell SNARE complex is regulated by accessory binding proteins, such as double C2 domain–containing protein β (Doc2b). Upon glucose stimulation, STX binds VAMP2, permitting SNARE complex assembly and fusion of insulin granules with the plasma membrane (21,22). Doc2b is essential for this mechanism to occur (22–24).

We recently showed that Doc2b levels are reduced in the residual islet β-cells from new-onset human type 1 diabetes donor pancreata; Doc2b deficiency was recapitulated by treatment of nondiabetic human islets with proinflammatory cytokines, ex vivo (25). Proinflammatory cytokines are used to mimic the diabetogenic milieu by promoting loss of β-cell mass, given that loss of β-cell mass in the context of type 1 diabetes is linked to apoptosis (26,27). Whether Doc2b plays a role in β-cell survival or apoptosis remains unknown.

Doc2b is a ubiquitously expressed, 46–50-kDa protein that localizes to the plasma membrane in β-cells and muscle/fat cells (22,28,29). Doc2b contains an N-terminal Munc13-interacting domain (MID) linked to C-terminal tandem C2 domains (C2A and C2B), which are motifs known to bind Ca^{2+} and phospholipids. Several laboratories have shown that overexpression of Doc2b enhances insulin secretion by 30–40% in vitro (24,29). Moreover, transgenic mice overexpressing Doc2b (simultaneously in the pancreas, skeletal muscle, and adipose tissue) show enhanced whole-body glucose homeostasis and insulin sensitivity, with enhanced islet glucose-stimulated insulin secretion (GSIS) ex vivo, but have normal fasting insulin levels (28). These data suggest that Doc2b enrichment is beneficial, although the investigation of detailed mechanisms for Doc2b actions in the β-cells has been limited by the use of a global transgene expression system. Doc2b-null knockout mice harbor dysfunctional islets (30,31), consistent with the observed low Doc2b transcript levels in islets of diabetic rodents (25,32). However, it remains unknown whether Doc2b deficiency is causal or consequential to the loss of β-cell function and diabetes onset.

In this study, we tested the hypothesis that Doc2b deficiency underlies β-cell dysfunction and susceptibility to diabetes and that selective β-cell Doc2b enrichment is sufficient to confer protection against proinflammatory stimuli. Data gained from classic whole-body Doc2b heterozygous knockout mice, inducible β-cell–specific transgenic Doc2b overexpressing (βDoc2b-dTg) mice, and Doc2b overexpression in clonal β-cells provide strong support for this hypothesis. Furthermore, we show that enrichment of a peptide containing the Doc2b tandem C2 domains (C2AB) is sufficient to confer the GSIS-boosting effect of full-length Doc2b and protects against thapsigargin-induced β-cell apoptosis.

RESEARCH DESIGN AND METHODS

Materials

The rabbit anti-Doc2b antibody used for detection of endogenous Doc2b levels and detection of hDoc2b-DDK was purchased from Proteintech (1:1,000 dilution, catalog no. 20574–1-AP; Rosemont, IL). The rabbit anti-cMyc antibody (1:1,000 dilution, catalog no. sc-40) and mouse antiglucagon (1:200 dilution, catalog no. sc-13091) antibodies were purchased from Santa Cruz Biotechnology (Dallas, TX). The rabbit anti-STX4 antibody used in the pulldown binding assay was generated in house (33). Antibodies to cleaved caspase 3 (CC3; 1:1,000 dilution, catalog no. 9661), CHOP (1:1,000 dilution, catalog no. 2895), PARP (1:1,000 dilution, catalog no. 9532), phospho-eIF2a (p-eIF2a), and total eIF2a (1:1,000 dilution, catalog nos. 9721 and 9722, respectively) were purchased from Cell Signaling (Danvers, MA). The tubulin antibody was purchased from Abcam (1:5,000 dilution, catalog no. ab56676; Cambridge, MA). The guinea pig anti-insulin was from Dako/Agilent (1:100 dilution, catalog no. A0564; Santa Clara, CA). The goat anti-rabbit- and anti-mouse-horseradish peroxidase secondary antibodies were purchased from Bio-Rad (catalog nos. 1706515 and 1706516, respectively; Hercules, CA). Thapsigargin was purchased from Sigma-Aldrich (catalog no. T9033). Glutathione sepharose 4B agarose beads were obtained from GE Life Sciences (Pittsburgh, PA). Enhanced chemiluminescence was purchased from Amersham Biosciences (Pittsburg, PA). Humulin R was obtained from Eli Lilly and Co. (Indianapolis, IN). The rat (r)Doc2b-GFP and rC2AB-GFP plasmids were gifts from U. Ashery (Tel-Aviv University, Ramat-Aviv, Israel). The rat CaMut-GFP plasmid was a gift from E. Chapman (University of Wisconsin).

Animals and In Vivo Experiments

Animals were maintained under protocols approved by the Institutional Animal Care and Use Committees at Indiana University School of Medicine and the City of Hope, according to the Guidelines for the Care and Use of Laboratory Animals. $Doc2b^{+/-}$ knockout mice were generated as described previously (30). The rat Doc2b cDNA tagged with a C-terminal myc-his tag was subcloned into the 5′ *Pme*1 and 3′ *Bam*H1 restriction sites in the pTRE-pIRES-eGFP vector (gift from Drs. S. Afelik and J. Jenssen, Cleveland Clinic), downstream of the tetracycline response element (TRE), to provide tetracycline/doxycycline (Dox) inducibility. The linearized plasmid was microinjected into C57BL/6J oocytes (Transgenic Core, Indiana University School of Medicine). Of two founders, one transmitted the transgene to offspring and was shipped to the City of Hope Animal Research Center for colony expansion. TRE-$Doc2b^{-/+}$ offspring crossed to rat insulin promoter (RIP)–$rtTA^{-/+}$ mice (purchased from Jax Laboratories) produced Dox-inducible β-cell–selective expression in the double transgenic offspring (βDoc2b-dTg) mice. The mice were generated and maintained on the C57BL/6J genetic background.

Female βDoc2b-dTg mice and single transgenic controls were fasted for 6 h (0800–1400 h) before the intraperitoneal

glucose tolerance test (IPGTT; 2 mg/mL of glucose) and intraperitoneal insulin tolerance test (IPITT, insulin dose = 0.75 units/kg body weight), as previously described (30). Male Doc2b$^{+/-}$ and wild-type (Wt) littermate mice (7 weeks old) were used for streptozotocin (STZ) studies; a pre-STZ IPGTT was performed on day 0. On days 1–5, mice were injected intraperitoneally in multiple low doses with freshly prepared STZ (35 mg/kg body weight, as previously described [34]). A post-STZ IPGTT was performed on day 10. Male mice were used for STZ experiments, as they are reportedly more sensitive to STZ treatment (35). Male βDoc2b-dTg mice (aged 9–10 weeks) were provided Dox-treated (2 mg/mL) or standard drinking water for 3 weeks prior to multiple-low-dose (MLD) STZ (35–40 mg/kg doses); IPGTT was assessed on day 24. On day 25, serum samples and tissues were collected, and the pancreata were fixed and paraffin embedded for TUNEL staining. Non–STZ-treated male and female mice were used for tissue harvest and evaluation of protein/mRNA expression. Serum insulin levels were measured via radioimmunoassay (Millipore).

Immunofluorescence and TUNEL Staining

Paraffin-embedded pancreatic tissue sections were prepared and assessed as previously described (36). To assess β-cell specificity, pancreatic sections were immunostained with guinea pig anti-insulin (1:100, catalog no. A0564; DAKO, Agilent Technologies, Santa Clara, CA), rabbit anti-myc (1:100, catalog no. C3956; Sigma-Aldrich, St. Louis, MO), and mouse anti-glucagon (1:100, catalog no. G2654; Sigma-Aldrich). Alexa Fluor 568 goat anti-rabbit (1:200, catalog no. A11011; Thermo Fisher Scientific), 488 goat anti-guinea pig (1:100, catalog no. A11073; Thermo Fisher Scientific), and 647 goat anti-mouse IgG (Heavy + Light Chains [H+L], 1:100, catalog no. A21236; Thermo Fisher Scientific) were used to detect myc, insulin, and glucagon, respectively. Slides were counterstained to mark the nuclei using 4′,6-diamidino-2-phenylindole (DAPI) (Vectashield; Vector Laboratories, Burlingame, CA) and viewed using a Keyence BZ X-700 fluorescence microscope (Leica Microsystems, Deerfield, IL), and images were acquired using the 20× objective. To assess GLUT2 staining, pancreatic sections were immunostained with goat anti-GLUT2 (1:100, catalog no. sc-7580; Santa Cruz Biotechnology, Inc., Dallas, TX) and guinea pig anti-insulin (1:100, catalog no. A0564; DAKO, Agilent Technologies). Cy3 anti-goat (1:200, catalog no. 715-166-147, Jackson ImmunoResearch) and Alexa Fluor 488 goat anti-guinea pig (1:100, catalog no. A11073; ThermoFisher Scientific, Waltham, MA) were used to detect GLUT2 and insulin, respectively.

To assess apoptosis, the pancreatic sections were immunostained with guinea pig anti-insulin, and the TUNEL In Situ Cell Death Detection Kit, Fluorescein (Roche, Mannheim, Germany) was used to stain apoptotic cells. The Alexa Fluor 488 goat anti-guinea pig IgG (H+L) (1:500 dilution, catalog no. A11073; Thermo Fisher Scientific) secondary antibody was used for detection of insulin. Sections were scanned using the Zeiss Axio Observer and LSM 700 microscopes and analyzed using Image-Pro Software (Media Cybernetics, Rockville, MD). The results are expressed as the percentage of cells positive for TUNEL staining relative to the total number of insulin-positive cells.

Cell Culture, Transfections, GSIS, and Binding Assays

Human Doc2b (hDoc2b) adenovirus was generated by insertion of the hDoc2b-mycDDK cDNA from the pCMVhDoc2bmycDDK plasmid (OriGene Technology, Inc., Rockville, MD) into the pAd5CMVmpA adenoviral vector. The adenoviruses were packaged with EGFP to enable visualization of infection efficiency, and then were amplified and purified for use by Viraquest, Inc. (North Liberty, IA). Rat INS-1 832/13 β-cells (gift from C.B. Newgard, Duke University, Durham, NC, and P. Fueger, City of Hope; passage 70–80) were cultured in RPMI 1640 medium as previously described (37) and transduced with Ad5-CMV-hDoc2b prior to treatment with a cytokine mixture (10 ng/mL TNF-α, 100 ng/mL IFN-γ, and 5 ng/mL IL-1β; ProSpec, East Brunswick, NJ) for 16 h, as previously described (38). For evaluation of thapsigargin-induced apoptosis, INS-1 832/13 β-cells were transfected with rDoc2b-GFP, rC2AB-GFP, and rCaMut-GFP. Cells were transfected using the K2 Transfection System (Biontex, Munchen, Germany) and treated with 1 μmol/L thapsigargin for 6 h prior to harvest; concurrently, cells were treated with 1 mmol/L EGTA as a negative control. The cells were harvested in 1% NP-40 lysis buffer, and cleared detergent lysates were used for immunoblotting for apoptosis/endoplasmic reticulum (ER) stress markers.

Glutathione S-transferase (GST)–VAMP2 interaction assays were conducted as previously described (33). In brief, GST-VAMP2 protein conjugated to sepharose beads was mixed with cleared detergent cell lysates prepared from MIN6 β-cells that had been preincubated in serum-free media for 2 h and were harvested in 1% NP-40 lysis buffer, as previously described (39). Recombinantly expressed and purified Doc2b protein or C2AB peptide were added to the reactions, and reactions were rotated at 4°C for 2 h, beads were pelleted, and proteins were eluted for resolution on SDS-PAGE and immunoblotting.

GSIS analysis was performed as previously described (38). In brief, rat INS-1 832/13 β-cells and MIN6 β-cells were prepared for GSIS analysis using the K2 Transfection System (Biontex). INS-1 832/13 cells were placed in low-glucose/low-serum medium overnight prior to starvation in Krebs-Ringer bicarbonate buffer for 1 h and treated with glucose (basal: 2.8 mmol/L; glucose stimulated: 20 mmol/L) for 30 min. The MIN6 cells were serum starved in modified Krebs-Ringer bicarbonate buffer for 1 h prior to glucose treatment (basal: 2.8 mmol/L; glucose stimulated: 20 mmol/L). The supernatants were collected for measurement of insulin content using the Rat Insulin ELISA (Mercodia, Uppsala, Sweden) or Mouse Insulin ELISA (Alpco, Salem, NH).

Quantitative Real-time PCR

Total RNA was isolated from mouse islets, hypothalamus, and cerebellum using the Qiagen RNAeasy Plus Mini Kit (Qiagen, Valencia, CA) and assessed using the QuantiTect SYBR Green RT-PCR kit (Qiagen). Primers used for the detection of rDoc2b-myc are as follows: forward 5′-ACTGTCTGAAGAACAAGGACAAGAG-3′ and reverse 5′-GAGTTTTTGTTCTACGTAAGCTTGG-3′. Hypoxanthine-guanine phosphoribosyltransferase primers were used for normalization: forward 5′-AAGCCTAAGATGAGCGCAAG-3′ and reverse 5′-TTACTAGGCAGATGGCCACA-3′. Primers used for the detection of rat/mouse Doc2b (nontagged) are as follows: forward 5′-CCAGCAAGGCAAATAAGCTC-3′ and reverse 5′-GTTGGGTTTCAGCTTCTTCA-3′.

Islet Morphometry

Islet morphometry was conducted using anti-insulin–stained pancreatic sections, as previously described (38). The percentage of β-cell area was calculated using Keyence BZX-Analyzer software (Keyence Corporation, Itasca, IL). The data shown are representative of three pancreatic sections per mouse. The β-cell mass was calculated by multiplying the percentage of the β-cell area by the pancreas weight.

Statistical Analysis

All data are expressed as the mean ± SD for all figures, except those representing IPGTT/IPITT or area under the curve (AUC) (mean ± SEM). The data were evaluated for statistical significance using Student *t* test for comparison of two groups, or ANOVA and Tukey post hoc test (GraphPad Software, La Jolla, CA) for more than two groups.

RESULTS

Doc2b$^{+/-}$ Mice Are Highly Susceptible to STZ-Induced Glucose Intolerance

To assess whether Doc2b abundance impacts β-cell susceptibility to diabetogenic insults, we studied Doc2b$^{+/-}$ mice prior to and after MLD-STZ induction of diabetes. Prior to MLD-STZ treatment, young 7-week-old male Doc2b$^{+/-}$ and Wt littermate mice showed no differences in blood glucose levels (Fig. 1*A* and *B*) and β-cell mass and harbored the expected 50% reduction in Doc2b protein (Supplementary Fig. 1*A* and *B*). Ten days after the first STZ injection, the Doc2b$^{+/-}$ mice showed significantly higher blood glucose levels than Wt mice (Fig. 1*C* and *D*). One day later, all pancreata were collected and processed for TUNEL staining, and the Doc2b$^{+/-}$ mice showed greater than threefold higher levels of β-cell apoptosis than the Wt mice (Fig. 1*E*). Although the number of islets was similar in the Doc2b$^{+/-}$ and Wt mice, the percentage of the islet area occupied by β-cells was decreased in the Doc2b$^{+/-}$ mice, which also resulted in a reduced β-cell mass (Fig. 1*F* and *G*). Consistent with this, serum insulin levels in the Doc2b$^{+/-}$ were lower than Wt mice post-STZ treatment, whereas prior to STZ, levels were similar to Wt mice (Supplementary Fig. 2). The body weights of Doc2b$^{+/-}$ and Wt mice were equivalent before and after the brief STZ treatment (Supplementary Table 1).

Enhanced Glucose Tolerance in Doxycycline-Inducible β-Cell–Specific Doc2b-Overexpressing Transgenic Mice

To determine whether β-cell–specific overexpression of Doc2b is sufficient to enhance whole-body glucose tolerance, we generated a Dox-induced, β-cell–specific double transgenic mouse model (βDoc2b-dTg) (Fig. 2*A*). The Doc2b mRNA abundance in islets isolated from female mice was approximately four- to fivefold higher in Dox-induced βDoc2b-dTg mice (same for male mice, data not shown) than in non–Dox-treated βDoc2b-dTg control mice (Fig. 2*B* and Supplementary Fig. 3), and the presence of the myc-tagged Doc2b protein was clearly detectable (Fig. 2*C*). No transgene overexpression was detected in the hypothalamus or cerebellum, indicating no aberrant expression due to the RIP-rtTA (Fig. 2*D*). Immunofluorescent analysis of βDoc2b-dTg islets shows β-cell–specific overexpression of Doc2b-myc in Dox-treated βDoc2b-dTg mice (Fig. 2*E*).

Changes to whole-body glucose homeostasis were assessed by IPGTT in the βDoc2b-dTg mice. Dox-induced dTg mice showed significantly lower blood glucose levels (i.e., improved glucose tolerance) after glucose injection; basal fasting blood glucose levels were similar to those of non–Dox-treated dTg control mice (Fig. 3*A* and *B*) or single transgenic mice (Supplementary Fig. 4). Consistent with this, the serum insulin levels in Dox-treated βDoc2b-dTg mice were higher than controls within the first 10 min after glucose injection during IPGTT, but they were not statistically different under basal (time 0 in the IPGTT) conditions (Fig. 3*C*). No differences were seen between Dox-treated and non–Dox-treated βDoc2b-dTg mice in IPITTs, suggesting no changes to peripheral insulin sensitivity (Fig. 3*D* and *E*). βDoc2b-dTg mice had similar body weight and tissue weights relative to the control Dox^{+} or noninduced (Dox^{-}) single transgenic mice and noninduced dTg mice (Supplementary Table 2). These data suggest that enrichment of Doc2b selectively in adult pancreatic islet β-cells is sufficient to improve whole-body glucose homeostasis.

βDoc2b-dTg Mice Are Protected From STZ-Induced Glucose Intolerance and β-Cell Apoptosis

Male βDoc2b-dTg mice were subjected to a longer (24-day) MLD-STZ protocol to determine if β-cell Doc2b enrichment protects islets from diabetogenic stress. IPGTT assessments at 24 days after initiation of the STZ protocol reveal increased blood glucose levels, with fasting levels ~300 mg/dL in non–Dox-treated dTg mice (Fig. 4*A* and *B*). In contrast, Dox-induced βDoc2b-dTg mice were largely protected, even though the longer time after STZ treatment would be expected to increase β-cell destruction. Body weights of the Dox^{+} and non–Dox-treated mice were similar both before and after MLD-STZ treatment (Supplementary Table 3).

To determine if the improved glucose tolerance, robust serum insulin response, and protection from STZ-induced glucose intolerance in the βDoc2b-dTg mice were related

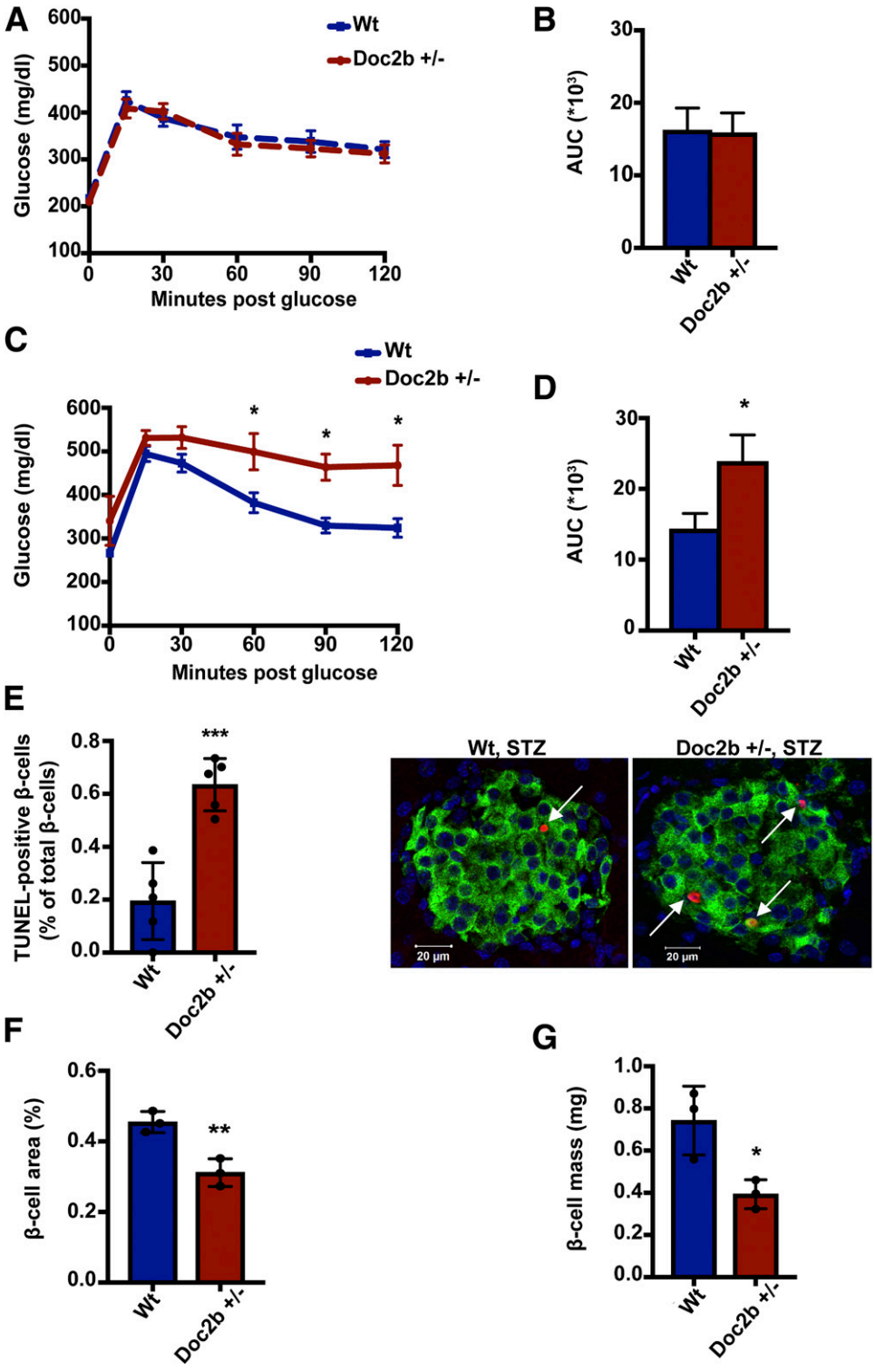

Figure 1—Doc2b$^{+/-}$ deficient mice are more susceptible to STZ-induced glucose intolerance and β-cell apoptosis. *A*: Prior to treatment with STZ (day 0), young 7-week-old male Wt and Doc2b$^{+/-}$ mice were fasted 6 h and subjected to IPGTT; n = 13 mice/group. *B*: Quantification of AUC for pre-STZ IPGTT. *C*: Doc2b$^{+/-}$ and Wt littermates were then injected daily on days 1–5 with STZ (35 mg/kg body weight), and on day 10 were subjected to a post-STZ IPGTT; n = 8 mice/group. *D*: Quantification of AUC for post-STZ IPGTT. *E*: TUNEL immunofluorescence staining and quantification of TUNEL-positive β-cells (indicated by arrows in images, expressed as % of total β-cells) were conducted on fixed pancreas sections from STZ-treated Doc2b$^{+/-}$ and Wt mice; n = 5 mice/group. Bar = 20 μm. Islet β-cell area (*F*) and islet β-cell mass (*G*) were calculated from fixed Doc2b$^{+/-}$ and Wt pancreata immunostained for insulin content; n = 3 mice/group (three sections per mouse). Data for *A–D* are shown as mean ± SEM and for *E–G* as mean ± SD. $^{*}P < 0.05$; $^{**}P < 0.01$; $^{***}P < 0.001$.

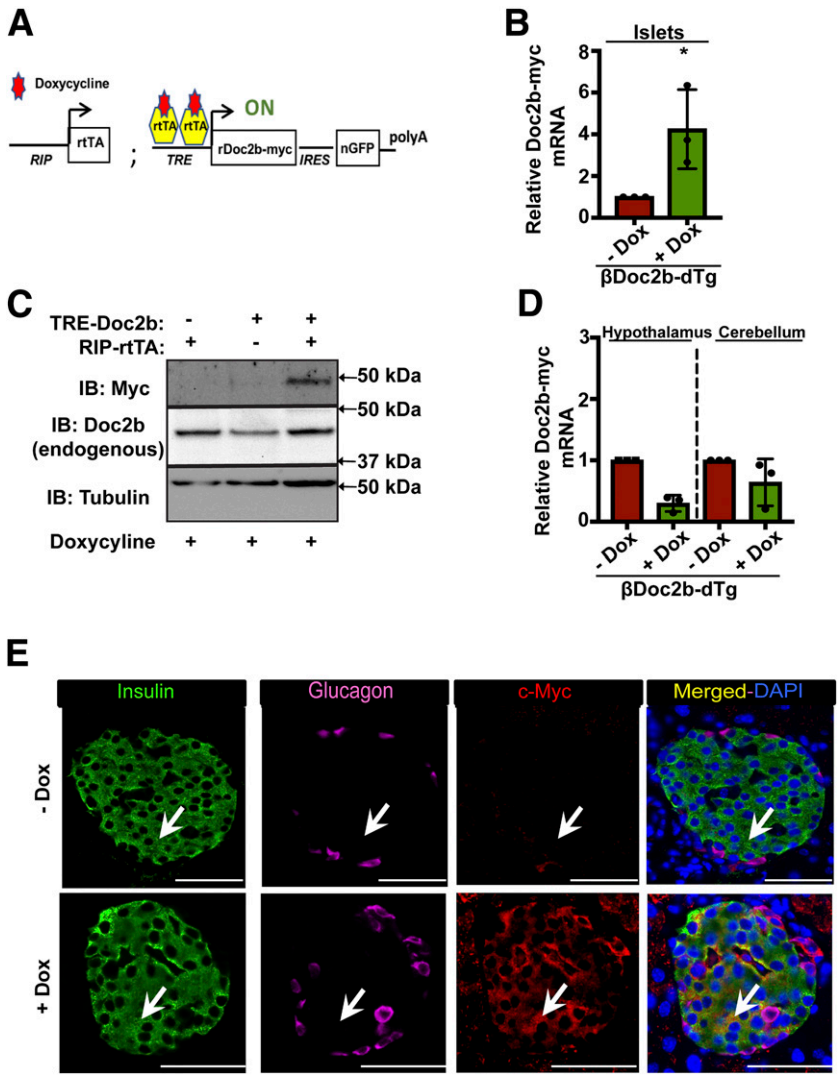

Figure 2—Generation of βDoc2b-dTg mice. *A*: Schematic design of RIP-rtTA$^{-/+}$ mice crossed to new TRE-Doc2b$^{-/+}$ mice. *B*: rDoc2b-myc mRNA, in islets isolated from female double transgenic (βDoc2b-dTg) mice. Dox-induced expression of Doc2b-myc and endogenous Doc2b protein in isolated islets (*C*) and lack of overexpression of rDoc2b-myc mRNA in the hypothalamus or cerebellum of the βDoc2b-dTg mice (*D*). IB, immunoblot. *E*: Immunofluorescence imaging of Doc2b overexpression in the islets of βDoc2b-dTg mice treated with or without Dox. Arrows denote the same position in each horizontal panel to show positive or negative c-Myc staining within a β-cell. Shown are the mean ± SD of at least three mice per group. *$P < 0.05$. Bar = 50 μm.

to changes in β-cell apoptosis, pancreata from the STZ-treated dTg mice were assessed by TUNEL staining. Islets from Dox-treated βDoc2b-dTg mice contained ~58% fewer apoptotic cells than islets from non–Dox-treated dTg mice (Fig. 4*C*). Although the islet numbers were similar in both groups (data not shown), the Dox-treated βDoc2b-dTg mice had a larger β-cell area, corresponding to higher β-cell mass, compared with non–Dox-treated dTg mice (Fig. 4*D* and *E*). Consistent with this, Dox-induced dTg mice had serum insulin levels similar to Wt mice pre-STZ, whereas non–Dox-treated dTg mice showed loss of insulin (Supplementary Fig. 5). GLUT2 expression in Dox^{+} and Dox^{-} βDoc2b-dTg mice was unchanged (Supplementary Fig. 6). These data suggest that overexpression of Doc2b protects islet β-cells against STZ-induced β-cell death.

Doc2b Overexpression Protects Against Cytokine-Induced Apoptosis and Reduces ER Stress

To date, all studies of Doc2b overexpression in islets and in vivo function have used rat Doc2b; hDoc2b has yet to be tested. Toward this, we generated adenoviral particles encoding hDoc2b tagged on the C terminus with DDK. Ad-hDoc2b-DDK was packaged with GFP and was detected in ≥70% of rat INS-1 832/13 cells after viral transduction (Supplementary Fig. 7); the Ad vector control transduced ~100% of cells. Treatment of Ad-hDoc2b–expressing INS-1 832/13 cells with proinflammatory cytokines for 16 h resulted in a 45% reduction in CC3 and >50% reduction in cleaved PARP, as compared with control cells (Fig. 5). Additionally, the levels of ER stress markers CHOP and p-eIF2a were reduced by ~50% and ~60%, respectively, in Doc2b-overexpressing

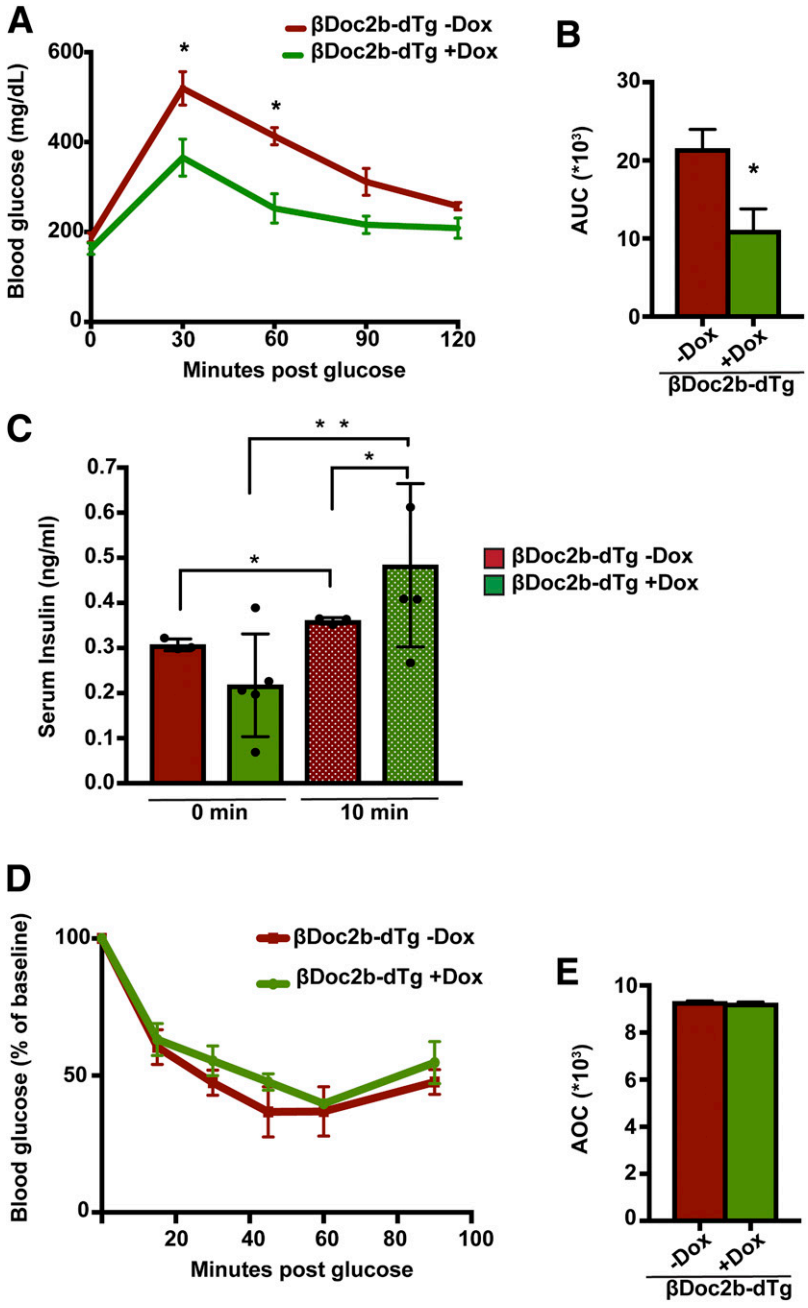

Figure 3—βDoc2b-dTg mice have enhanced glucose tolerance and glucose-stimulated serum insulin content. *A*: Female βDoc2b-dTg mice at 12–13 weeks of age were fasted 6 h and subjected to an IPGTT; $n = 5$ mice/group. *B*: Quantification of the AUC for IPGTT. *C*: Serum insulin content in mice fasted for 6 h (0 min) and 10 min after a glucose injection; $n = 3$–5 sets of mice. *D*: Female βDoc2b-dTg mice were fasted 6 h and subjected to an IPITT; $n = 4$ βDoc2b-dTg Dox^- and $n = 3$ βDoc2b-dTg Dox^+ mice. *E*: Area over the curve (AOC) analyses of the IPITT. Data for *A*, *B*, *D*, and *E* are shown as mean ± SEM and for *C* are shown as mean ± SD. $^*P < 0.05$; $^{**}P < 0.01$.

β-cells (Fig. 5). These data show that Doc2b protects cells from apoptotic stimuli and reduces ER stress.

The Doc2b Peptide C2AB Is Sufficient to Protect Against Thapsigargin-Induced ER Stress Via Calcium Handling

Doc2b is composed of three primary domains, MID, C2A, and C2B (Fig. 6*A*); the C2 domains are known calcium-sensing domains, binding two calcium ions each and contributing to Doc2b's function. To further investigate Doc2b's antiapoptotic actions and the role of the C2 domains in alleviating ER stress, GFP-tagged plasmids were generated that encode rDoc2b (Doc2b-GFP), a fragment containing an N-terminal truncation of the MID domain (C2AB-GFP), and CaMut-GFP, a mutated form of Doc2b-GFP carrying D→N substitutions in the amino acids implicated in calcium handling in the C2 domains (40)

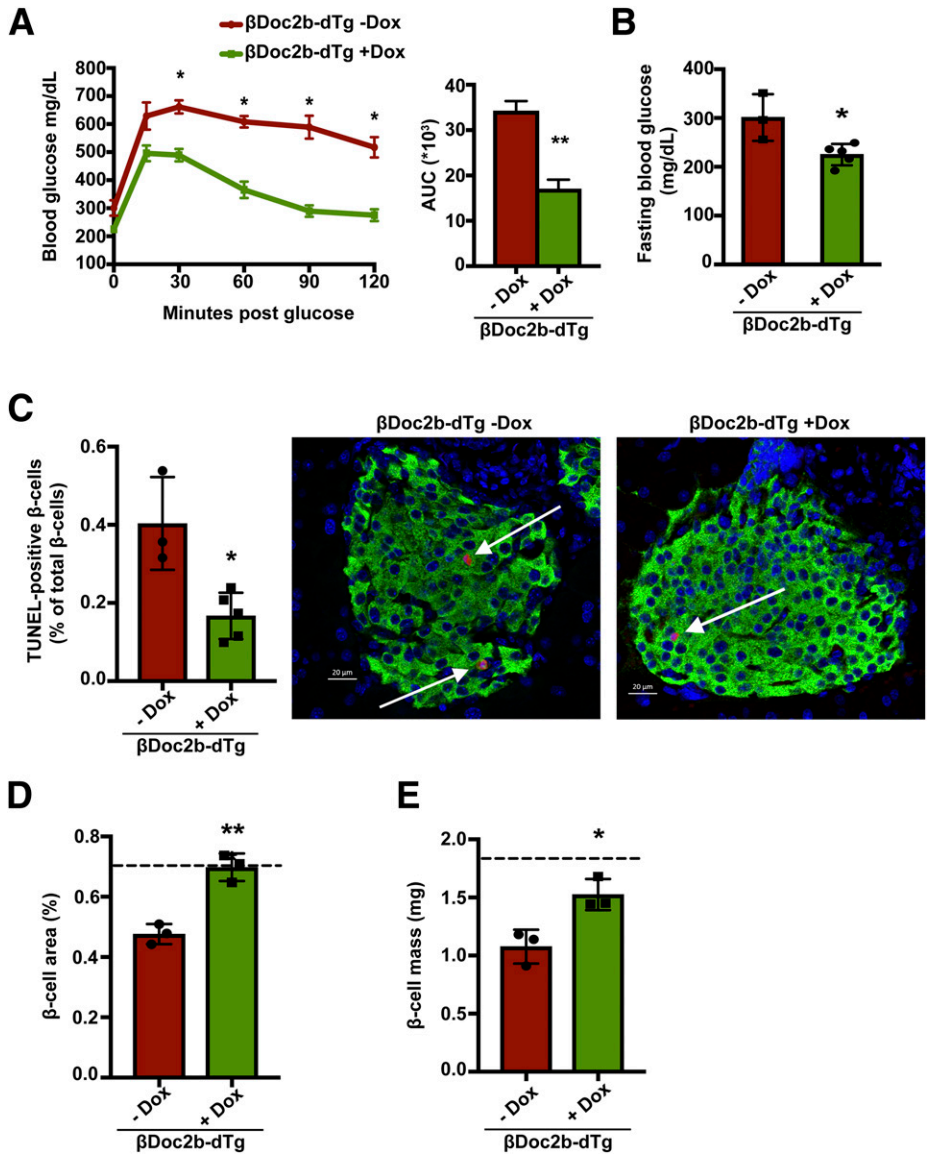

Figure 4— βDoc2b-dTg mice are protected from STZ-induced glucose intolerance, fasting hyperglycemia, and β-cell apoptosis. *A*: Male βDoc2b-dTg mice aged 12–13 weeks were injected daily on days 1–5 with STZ (35–40 mg/kg body weight), and on day 24 were fasted 6 h and subjected to an IPGTT. AUC quantification for IPGTT; $n = 3$ βDoc2b-dTg Dox$^-$ and $n = 5$ βDoc2b-dTg Dox$^+$ mice. *B*: Fasting blood glucose of STZ-treated βDoc2b-dTg mice; $n = 3$ βDoc2b-dTg Dox$^-$ and $n = 5$ βDoc2b-dTg Dox$^+$ mice. *C*: Immunofluorescence staining and quantification of TUNEL-positive β-cells (indicated by arrows in images, expressed as % of total β-cells) were conducted on fixed pancreata of βDoc2b-dTg Dox$^-$ and βDoc2b-dTg Dox$^+$ mice; $n = 3$ βDoc2b-dTg Dox$^-$ and $n = 5$ βDoc2b-dTg Dox$^+$. Bar = 20 μm. Islet β-cell area (*D*) and islet β-cell mass (*E*) were calculated from fixed βDoc2b-dTg whole pancreata immunostained for insulin content. The dotted line indicates the β-cell area and mass of non–STZ-treated Wt mice in our colony (38); $n = 3$ mice/group (three sections per mouse). *$P < 0.05$; **$P < 0.01$. Data for *A* are shown as mean ± SEM and for *B*–*E* are shown as mean ± SD.

(Fig. 6*A*). INS-1 832/13 cells were treated with the ER stress inducer and SERCA2b pump inhibitor thapsigargin. Treatment of Doc2b-GFP– and C2AB-GFP–overexpressing INS-1 832/13 cells with 1 μmol/L thapsigargin for 6 h decreased the levels of CHOP and CC3, compared with control (GFP)-treated cells (Fig. 6*B*). These decreased levels were similar to the levels of CHOP in cells treated with the calcium chelator EGTA (Fig. 6*B*). The benefit of expressing Doc2b-GFP or C2AB-GFP was absent when the cells were transfected with the calcium binding–deficient mutant form of Doc2b, CaMut-GFP (Fig. 6*A* and *B*). These data suggest that Doc2b's calcium binding capacity within the C2AB tandem domains is linked to its protective effect against ER stress and apoptosis.

The Doc2b Peptide C2AB Is Sufficient to Enhance Insulin Exocytosis

Because the C2AB peptide was sufficient to protect β-cells against thapsigargin-induced apoptosis, we investigated the capacity of C2AB to enhance β-cell function. Full-length rDoc2b-GFP expression in MIN6 cells recapitulated

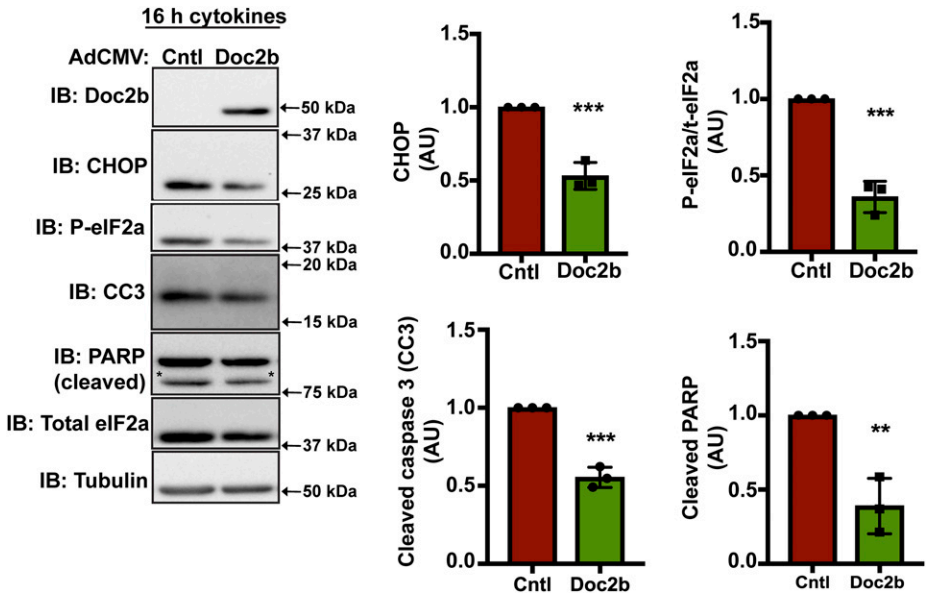

Figure 5—Doc2b overexpression in rat INS-1 832/13 cells protects against proinflammatory cytokine-induced β-cell apoptosis. Rat INS-1 832/13 were transduced with Ad5-CMV-hDoc2b-DDK or control virus (AdCMV, Cntl) and subsequently treated with a cocktail of proinflammatory cytokines (10 ng/mL TNF-α, 100 ng/mL IFN-γ, and 5 ng/mL IL-1β) for 16 h. Resultant cleared cell lysates were assessed for hDoc2b-DDK (~50 kDa, endogenous is 46 kDa) overexpression and effect upon CC3, CHOP, p-eIF2a/total eIF2a (t-eIF2a), and cleaved PARP levels. The asterisk in the immunoblot (IB) indicates the cleaved PARP band used for analysis. Tubulin serves as a protein loading control. Data represent the mean ± SD of three independent sets of cell lysates. $^{**}P < 0.01$; $^{***}P < 0.001$. AU, arbitrary units.

the enhancement of GSIS seen with rDoc2b in prior reports (24,28,29) (Fig. 7*A*). Remarkably, C2AB enhanced GSIS by approximately two- to threefold, similar to full-length Doc2b (Fig. 7*A*). Neither C2A or C2B expression alone enhanced GSIS, despite confirmed expression of each peptide; if anything, the C2AB-GFP protein expression levels were slightly lower than those of the other proteins (Fig. 7*B*). The insulin content was also similar among all treatment groups (Supplementary Fig. 8*A*). These results were recapitulated when the constructs were tested in INS-1 832/13 cells (Fig. 7*C* and *D* and Supplementary Fig. 8*B*). Doc2b is required for SNARE complex formation in β-cells, possibly via increasing STX4 activation (i.e., interaction with its cognate v-SNARE partner, VAMP2 [28]). To determine if C2AB can replicate the underlying mechanism, the C2AB and Doc2b proteins (untagged) were tested for the ability to increase STX4 binding to GST-VAMP2 (Fig. 7*E*). Notably, the C2AB protein fully recapitulated the Doc2b-induced activation of STX4. These data suggest that C2AB includes a minimal region of Doc2b that is sufficient to confer enhanced GSIS, STX4 activation, and protection against apoptosis.

DISCUSSION

The data presented here demonstrate an important role for Doc2b in maintaining β-cell mass and function. We propose that Doc2b deficiency leaves β-cells more susceptible to diabetogenic damage and that overexpression of Doc2b in the β-cell enhances whole-body glucose homeostasis and prevents β-cell apoptosis and ER stress. We also show that C2AB comprises a minimal Doc2b region that is required for enhanced insulin secretion and that its antiapoptotic effects are linked to known sites of calcium binding within the C2AB region. Hence, delivery of C2AB could represent a novel candidate therapeutic strategy to promote and protect functional β-cell mass.

To our knowledge, this study is the first report showing protective, antidiabetic properties of Doc2b. We found that reducing the Doc2b levels in mice ($Doc2b^{+/-}$) increases susceptibility to MLD-STZ–induced β-cell destruction and glucose intolerance. On the other hand, enhancing Doc2b levels in the β-cell (βDoc2b-dTg) decreases susceptibility to MLD-STZ–induced β-cell destruction and glucose intolerance. INS-1 832/13 β-cells transduced to overexpress hDoc2b also exhibit protection from proinflammatory cytokine and thapsigargin-induced apoptosis, indicating that Doc2b protection occurs at the level of the β-cells, and the protective effect is not dependent upon interislet non–β-cell communication, nor is it due to a circulating factor in vivo. The role of Doc2b or other exocytosis proteins in β-cell survival mechanisms still remains largely unexplored; however, recent reports have shown involvement of exocytosis proteins, such as VAMP8, in β-cell proliferation (20). Also, in neurons, Doc2b has been implicated in proliferation and differentiation during early embryogenesis (41,42). However, the β-cell area and insulin content in islets from mice with increased or decreased Doc2b levels are similar to Wt mice without diabetogenic stimuli (28,30,31); these data do not support the hypothesis that Doc2b overexpression acts

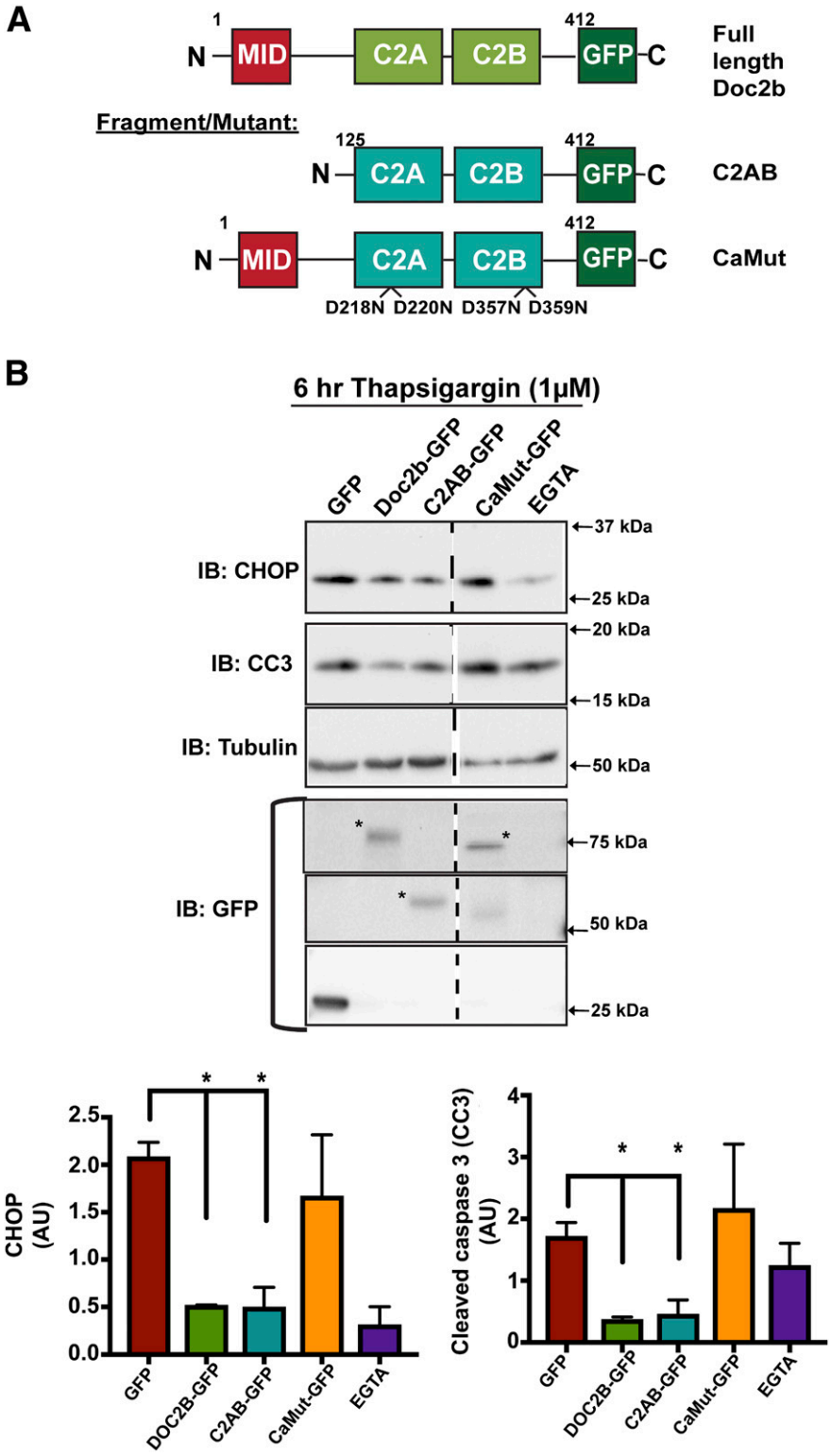

Figure 6—Ability of Doc2b and the N-terminal truncation product C2AB to protect against ER stress via calcium handling. *A*: Schematic of the rDoc2b-GFP truncation and mutation constructs. The numbers above each construct refer to the N- and C-terminal amino acids in each of the GFP fusion proteins. *B*: INS-1 832/13 cells were transfected with plasmid DNAs shown in *A*, and 48 h later, cells were treated with 1 μm thapsigargin for 6 h in complete media. Cells were harvested in lysis buffer and proteins resolved by SDS-PAGE for immunoblotting (IB) to detect the proteins noted in the figure. CHOP and CC3 are normalized to tubulin in each of three independent experiments. Asterisks in immunoblot denote the GFP fusion proteins; note that CaMut-GFP migrates slightly lower, as previously reported (40). Data represent the mean ± SD of three independent sets of homogenates. *$P < 0.05$. AU, arbitrary units.

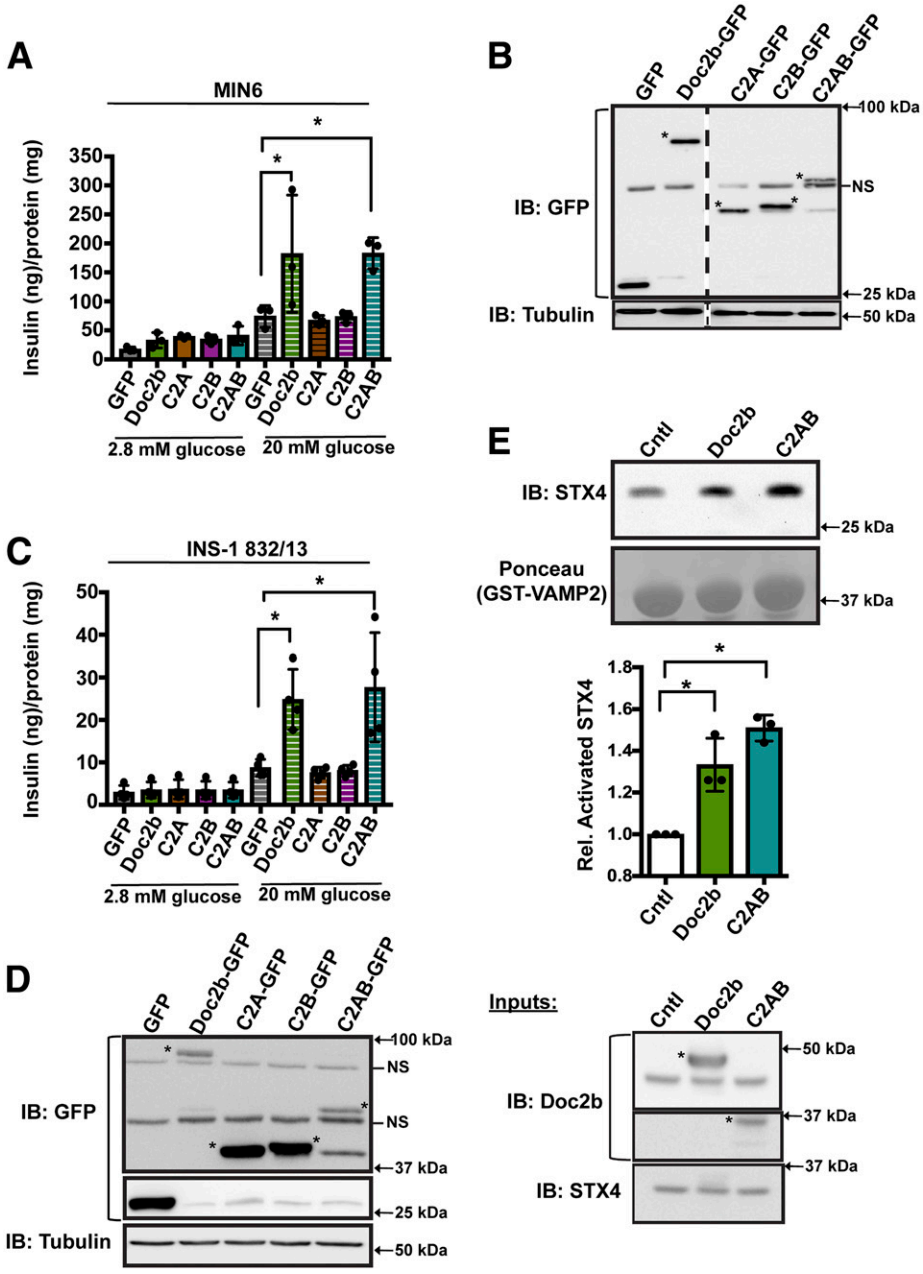

Figure 7— Ability of the C2AB peptide to mimic full-length Doc2b function in GSIS. *A*: GSIS in MIN6 cells expressing full-length rDoc2b-GFP, the N-terminal truncation mutant C2AB-GFP, and individual domains, C2A-GFP or C2B-GFP. *B*: Expression was confirmed by immunoblotting (IB). Asterisks in the immunoblots denote the presence of the Doc2b-GFP, C2A-GFP, C2B-GFP, and C2AB-GFP bands by their expected molecular weights. The vertical dashed line indicates splicing of lanes from within the same gel exposure. *C* and *D*: GSIS and protein expression of rDoc2b-GFP truncation mutants in INS-1 832/13 cells. Asterisks denote the C2A, C2B, and C2AB bands. *E*: Recombinant C2AB mimics the enhancement effect of full-length Doc2b protein (nontagged) upon STX4 activation in MIN6 cells. Data represent the mean ± SD of three independent sets of cell lysate in GST-VAMP2 pulldown assays. $^*P < 0.05$. Cntl, control; NS, nonspecific band.

via promoting proliferation or differentiation in the β-cell per se. The data reported here suggest that Doc2b overexpression promotes β-cell survival and protects β-cell mass from apoptosis and ER stress, with the protection occurring at the level of the β-cell itself. This hypothesis is supported by our data showing the antiapoptotic actions of hDoc2b overexpression in clonal β-cell lines.

Doc2b is a C2 domain–containing protein in a family of proteins that includes Munc13, synaptotagmins, ferlins, rabphilin 3A, and RIM1/2 (43–45). These proteins have two aspects in common: all are calcium regulated/calcium sensing, and all are implicated in vesicle trafficking/exocytosis. The role of Doc2b as a calcium sensor in β-cells has been reported (24), and the tandem C2 domain region of

Doc2b, referred to here as the C2AB, is sufficient to support membrane fusion in cell-free assays and shows stronger liposome binding than either of the isolated C2A and C2B domains (42). Indeed, our data show that C2AB can fully recapitulate the antiapoptotic effects of full-length Doc2b, likely through calcium handling. The CaMut form of C2AB has been previously reported to abolish Doc2b's calcium binding capacity (40). ER stress mechanisms are known to be calcium-dependent events, and thus we propose that Doc2b may sequester calcium, resulting in reduced CC3, PARP, CHOP, and p-eIF2a.

C2AB also recapitulated the GSIS enhancement seen with full-length Doc2b, whereas the C2 domains individually did not. Interestingly, the C2AB protein also recapitulated the activating effect of full-length Doc2b upon STX4, consistent with prior work showing Doc2b to promote SNARE protein assembly (21,23,24,46). C2AB may confer its SNARE complex–promoting effect, in part, by acting directly on the membrane, as recent work shows that C2AB is sufficient to assemble in a ring-like oligomer (47) and act directly on membranes to regulate hemifusion events in neurons (48). These findings are important starting points for further mechanistic investigation of how the exocytotic function of Doc2b might protect β-cell function.

In summary, the data presented here show a novel, antiapoptotic role for Doc2b in the β-cell. We propose that β-cell–specific overexpression of Doc2b is sufficient to enhance whole-body glucose homeostasis and to protect the β-cell mass against type 1 diabetes–related stress. Furthermore, we show that the tandem C2AB domain is sufficient to enhance insulin secretion and protect against apoptosis and that this may be due to calcium handling. Doc2b thus carries the potential to be a therapeutic target for prevention/management of type 1 diabetes.

Acknowledgments. The authors are grateful to Drs. Jeffrey Elmendorf, Carmella Evans-Molina, A.J. Baucum (all from Indiana University), and Patrick Fueger (now at City of Hope) for their sage advice and feedback on this project emanating from the doctoral dissertation of A.A. The authors also thank Drs. Edwin Chapman and Uri Ashery for the calcium ligand mutant (CaMut-GFP) and C2AB-GFP plasmids, respectively. The authors thank Jeff Rawson (City of Hope) and the City of Hope Islet Core for isolating the mouse islets used for this study. Dr. Nancy Linford (Linford Biomedical, Iceland) provided editing assistance.

Funding. This work was supported by grants from the American Heart Association (17POST33661194 to J.Z. and 15PRE21970002 to R.T.), the National Institutes of Health/National Institute of Diabetes and Digestive and Kidney Diseases (R01 DK067912 and R01 DK102233 to D.C.T.; Indiana CTSI Predoctoral Award funded in part by grant UL1TR001108 [A. Shekhar, PI] to A.A.), and JDRF (INO-2014-165-A-V to D.C.T.). Additional financial support was provided to D.C.T. from the Ruth and Robert Lanman Endowment, the George Schaeffer Award, and an Excellence Award through the City of Hope. Research reported in this publication also includes work performed in the Integrative Genomics Core, Drug Discovery and Structural Biology Core, Light Microscopy/Digital Imaging Core, Pathology Research Services Core, and the Comprehensive Metabolic Phenotyping Core (all affiliated with City of Hope), all supported by the National Cancer Institute of the National Institutes of Health under award number P30CA33572.

The content is solely the responsibility of the authors and does not necessarily represent the official views of the National Institutes of Health.

Duality of Interest. No potential conflicts of interest relevant to this article were reported.

Author Contributions. A.A. performed the majority of the studies, contributed to the discussion, and wrote and edited the manuscript. E.O. designed and generated the TRE-Doc2b mice and contributed to the discussion. E.M.O. assisted with in vivo studies, TUNEL staining, immunohistochemistry, and islet cell morphometrics. J.Z. performed quantitative real-time PCR analyses and contributed to discussion. M.A. generated the Doc2b adenovirus and contributed to discussion. A.S.M.M. assisted with immunofluorescent imaging of pancreata. R.T., V.A.S., and R.V. assisted with in vivo studies and contributed to the discussion. D.C.T. conceived of the study; contributed to the discussion; and wrote, reviewed, and edited the manuscript. All authors read and approved the final version of the manuscript. D.C.T. is the guarantor of this work and, as such, had full access to all the data in the study and takes responsibility for the integrity of the data and the accuracy of the data analysis.

Prior Presentation. Portions of this work were presented at the Levine-Riggs Symposium, Orlando, FL, 28–31 March 2017, and the 76th Scientific Sessions of the American Diabetes Association, New Orleans, LA, 10–14 June 2016.

References

1. Imperatore G, Boyle JP, Thompson TJ, et al.; SEARCH for Diabetes in Youth Study Group. Projections of type 1 and type 2 diabetes burden in the U.S. population aged <20 years through 2050: dynamic modeling of incidence, mortality, and population growth. Diabetes Care 2012;35:2515–2520

2. Mayer-Davis EJ, Lawrence JM, Dabelea D, et al.; SEARCH for Diabetes in Youth Study. Incidence trends of type 1 and type 2 diabetes among youths, 2002-2012. N Engl J Med 2017;376:1419–1429

3. Dabelea D, Mayer-Davis EJ, Saydah S, et al.; SEARCH for Diabetes in Youth Study. Prevalence of type 1 and type 2 diabetes among children and adolescents from 2001 to 2009. JAMA 2014;311:1778–1786

4. Ferrannini E, Mari A, Nofrate V, Sosenko JM, Skyler JS; DPT-1 Study Group. Progression to diabetes in relatives of type 1 diabetic patients: mechanisms and mode of onset. Diabetes 2010;59:679–685

5. Steffes MW, Sibley S, Jackson M, Thomas W. Beta-cell function and the development of diabetes-related complications in the diabetes control and complications trial. Diabetes Care 2003;26:832–836

6. Nathan DM, Genuth S, Lachin J, et al.; Diabetes Control and Complications Trial Research Group. The effect of intensive treatment of diabetes on the development and progression of long-term complications in insulin-dependent diabetes mellitus. N Engl J Med 1993;329:977–986

7. Nathan DM, Cleary PA, Backlund JY, et al.; Diabetes Control and Complications Trial/Epidemiology of Diabetes Interventions and Complications (DCCT/EDIC) Study Research Group. Intensive diabetes treatment and cardiovascular disease in patients with type 1 diabetes. N Engl J Med 2005;353:2643–2653

8. Gembal M, Gilon P, Henquin JC. Evidence that glucose can control insulin release independently from its action on ATP-sensitive K+ channels in mouse B cells. J Clin Invest 1992;89:1288–1295

9. Kiraly-Borri CE, Morgan A, Burgoyne RD, Weller U, Wollheim CB, Lang J. Soluble N-ethylmaleimide-sensitive-factor attachment protein and N-ethylmaleimide-insensitive factors are required for Ca2+-stimulated exocytosis of insulin. Biochem J 1996;314:199–203

10. Lang J. Molecular mechanisms and regulation of insulin exocytosis as a paradigm of endocrine secretion. Eur J Biochem 1999;259:3–17

11. Wheeler MB, Sheu L, Ghai M, et al. Characterization of SNARE protein expression in beta cell lines and pancreatic islets. Endocrinology 1996;137:1340–1348

12. Gaisano HY. Recent new insights into the role of SNARE and associated proteins in insulin granule exocytosis. Diabetes Obes Metab 2017;19(Suppl. 1):115–123

13. Aslamy A, Thurmond DC. Exocytosis proteins as novel targets for diabetes prevention and/or remediation? Am J Physiol Regul Integr Comp Physiol 2017;312:R739–R752

14. Ohara-Imaizumi M, Fujiwara T, Nakamichi Y, et al. Imaging analysis reveals mechanistic differences between first- and second-phase insulin exocytosis. J Cell Biol 2007;177:695–705

15. Sadoul K, Berger A, Niemann H, et al. SNAP-23 is not cleaved by botulinum neurotoxin E and can replace SNAP-25 in the process of insulin secretion. J Biol Chem 1997;272:33023–33027
16. Spurlin BA, Thurmond DC. Syntaxin 4 facilitates biphasic glucose-stimulated insulin secretion from pancreatic beta-cells. Mol Endocrinol 2006;20:183–193
17. Henquin JC, Nenquin M, Stiernet P, Ahren B. In vivo and in vitro glucose-induced biphasic insulin secretion in the mouse: pattern and role of cytoplasmic Ca2+ and amplification signals in beta-cells. Diabetes 2006;55:441–451
18. Xie L, Zhu D, Dolai S, et al. Syntaxin-4 mediates exocytosis of pre-docked and newcomer insulin granules underlying biphasic glucose-stimulated insulin secretion in human pancreatic beta cells. Diabetologia 2015;58:1250–1259
19. Rhodes CJ. *Processing of the Insulin Molecule*. LeRoith D, Simeon T, Olefsky J, Eds. Philadelphia, PA, Lippincott Williams & Wilkins, 2000
20. Zhu D, Zhang Y, Lam PP, et al. Dual role of VAMP8 in regulating insulin exocytosis and islet β cell growth. Cell Metab 2012;16:238–249
21. Ramalingam L, Lu J, Hudmon A, Thurmond DC. Doc2b serves as a scaffolding platform for concurrent binding of multiple Munc18 isoforms in pancreatic islet β-cells. Biochem J 2014;464:251–258
22. Jewell JL, Oh E, Bennett SM, Meroueh SO, Thurmond DC. The tyrosine phosphorylation of Munc18c induces a switch in binding specificity from syntaxin 4 to Doc2beta. J Biol Chem 2008;283:21734–21746
23. Yu H, Rathore SS, Davis EM, Ouyang Y, Shen J. Doc2b promotes GLUT4 exocytosis by activating the SNARE-mediated fusion reaction in a calcium- and membrane bending-dependent manner. Mol Biol Cell 2013;24:1176–1184
24. Miyazaki M, Emoto M, Fukuda N, et al. DOC2b is a SNARE regulator of glucose-stimulated delayed insulin secretion. Biochem Biophys Res Commun 2009;384:461–465
25. Aslamy A, Oh E, Ahn M, et al. Exocytosis protein DOC2B as a biomarker of type 1 diabetes. J Clin Endocrinol Metab 2018;103:1966–1976
26. Corbett JA, Wang JL, Sweetland MA, Lancaster JR Jr., McDaniel ML. Interleukin 1 beta induces the formation of nitric oxide by beta-cells purified from rodent islets of Langerhans. Evidence for the beta-cell as a source and site of action of nitric oxide. J Clin Invest 1992;90:2384–2391
27. Eizirik DL, Mandrup-Poulsen T. A choice of death–the signal-transduction of immune-mediated beta-cell apoptosis. Diabetologia 2001;44:2115–2133
28. Ramalingam L, Oh E, Thurmond DC. Doc2b enrichment enhances glucose homeostasis in mice via potentiation of insulin secretion and peripheral insulin sensitivity. Diabetologia 2014;57:1476–1484
29. Ke B, Oh E, Thurmond DC. Doc2beta is a novel Munc18c-interacting partner and positive effector of syntaxin 4-mediated exocytosis. J Biol Chem 2007;282:21786–21797
30. Ramalingam L, Oh E, Yoder SM, et al. Doc2b is a key effector of insulin secretion and skeletal muscle insulin sensitivity. Diabetes 2012;61:2424–2432
31. Li J, Cantley J, Burchfield JG, et al. DOC2 isoforms play dual roles in insulin secretion and insulin-stimulated glucose uptake. Diabetologia 2014;57:2173–2182
32. Keller MP, Choi Y, Wang P, et al. A gene expression network model of type 2 diabetes links cell cycle regulation in islets with diabetes susceptibility. Genome Res 2008;18:706–716
33. Wiseman DA, Kalwat MA, Thurmond DC. Stimulus-induced S-nitrosylation of Syntaxin 4 impacts insulin granule exocytosis. J Biol Chem 2011;286:16344–16354
34. Chen YC, Colvin ES, Griffin KE, Maier BF, Fueger PT. Mig6 haploinsufficiency protects mice against streptozotocin-induced diabetes. Diabetologia 2014;57:2066–2075
35. Leiter EH. Multiple low-dose streptozotocin-induced hyperglycemia and insulitis in C57BL mice: influence of inbred background, sex, and thymus. Proc Natl Acad Sci U S A 1982;79:630–634
36. Oh E, Kalwat MA, Kim MJ, Verhage M, Thurmond DC. Munc18-1 regulates first-phase insulin release by promoting granule docking to multiple syntaxin isoforms. J Biol Chem 2012;287:25821–25833
37. Hohmeier HE, Mulder H, Chen G, Henkel-Rieger R, Prentki M, Newgard CB. Isolation of INS-1-derived cell lines with robust ATP-sensitive K+ channel-dependent and -independent glucose-stimulated insulin secretion. Diabetes 2000;49:424–430
38. Ahn M, Yoder SM, Wang Z, et al. The p21-activated kinase (PAK1) is involved in diet-induced beta cell mass expansion and survival in mice and human islets. Diabetologia 2016;59:2145–2155
39. Oh E, Thurmond DC. The stimulus-induced tyrosine phosphorylation of Munc18c facilitates vesicle exocytosis. J Biol Chem 2006;281:17624–17634
40. Gaffaney JD, Xue R, Chapman ER. Mutations that disrupt Ca^{2+}-binding activity endow Doc2β with novel functional properties during synaptic transmission. Mol Biol Cell 2014;25:481–494
41. Korteweg N, Denekamp FA, Verhage M, Burbach JP. Different spatiotemporal expression of DOC2 genes in the developing rat brain argues for an additional, nonsynaptic role of DOC2B in early development. Eur J Neurosci 2000;12:165–171
42. Groffen AJ, Martens S, Díez Arazola R, et al. Doc2b is a high-affinity Ca2+ sensor for spontaneous neurotransmitter release. Science 2010;327:1614–1618
43. Friedrich R, Yeheskel A, Ashery U. DOC2B, C2 domains, and calcium: a tale of intricate interactions. Mol Neurobiol 2010;41:42–51
44. Duncan RR, Shipston MJ, Chow RH. Double C2 protein. A review. Biochimie 2000;82:421–426
45. Pinheiro PS, Houy S, Sørensen JB. C2-domain containing calcium sensors in neuroendocrine secretion. J Neurochem 2016;139:943–958
46. Fukuda N, Emoto M, Nakamori Y, et al. DOC2B: a novel syntaxin-4 binding protein mediating insulin-regulated GLUT4 vesicle fusion in adipocytes. Diabetes 2009;58:377–384
47. Zanetti MN, Bello OD, Wang J, et al. Ring-like oligomers of synaptotagmins and related C2 domain proteins. eLife 2016;5:e17262
48. Brouwer I, Giniatullina A, Laurens N, et al. Direct quantitative detection of Doc2b-induced hemifusion in optically trapped membranes. Nat Commun 2015;6:8387